Journal of Thermal Analysis and Calorimetry, Vol. 92 (2008) 1, 43–51

THERMAL STUDY OF POLYPYRROLE COMPLEXES WITH VERMICULITES OF DIFFERENT LAYER CHARGE

Veronica Ramírez-Valle[1*], *A. Lerf*[2], *F. E. Wagner*[3], *J. Poyato*[1] *and J. L. Pérez-Rodríguez*[1]

[1]Materials Science Institute of Seville, CSIC-US, Avd. Américo Vespucio 49, 41092 Sevilla, Spain
[2]Walther Meissner Institut, Bayerische Akademie der Wissenschaften, 85748 Garching, Germany
[3]Physik-Department, Technische Universität München, 95748 Garching, Germany

We have studied the synthesis of polypyrrole-clay nanocomposites by the in situ oxidative polymerization of pyrrole in the interlayer space of vermiculites with different layer charges from Santa Olalla and Ojén, Spain. Moreover, the influence of different interlayer cations (Na^+, Mg^{2+}, Fe^{3+}) on the interaction between pyrrole and the vermiculites was studied. The resulting materials were characterized by means of DTA-TG, XRD, FTIR and Mössbauer spectroscopy. In all samples polymerization of pyrrole was observed, presumably triggered by the structural iron. In most cases it was found to be externally deposited. An uptake of pyrrole in the interlayer space and PPy formation is observed in the case of the Fe^{3+}-intercalated Ojén vermiculite, which has a lower layer charge than the Santa Olalla vermiculite.

Keywords: *interlayer cation, nanocomposite, polymerization, polypyrrole, pyrrole, vermiculite*

Introduction

Since the first investigation devoted to the interaction of clays with polymers in the 1960's [1], the research on polymer-clay nanocomposites have grown into a separate branch of clay chemistry [2]. Only recently a new family of electroactive functional nanocomposites based on conducting polymers has been developed [3, 4].

Since the discovery of conducting organic polymers, their physicochemical properties as well as their possible applications have been the subject of many investigations [5]. Among all the different polymeric conductors polypyrrole (PPy) is one of the most interesting materials because of its high electronic and ionic conductivity, its interesting redox properties and a satisfactory environmental stability [6–11]. Due to these fortunate properties various applications have been proposed, for instance in batteries, supercapacitors, sensors, corrosion protection or artificial muscle fibers [8–13]. Moreover, PPy can be easily prepared by chemical or electrochemical oxidation of pyrrole (Py).

Like with other conducting polymers, some of the properties of PPy need to be improved, since its applicability is often impaired by chemical sensitivity and poor mechanical properties. One of the most efficient means of improving the properties or even of achieving new properties of PPy, is the preparation of PPy-based nanocomposites [11, 14–25]. Polymer-inorganic nanocomposites using smectites as the inorganic component exhibit a variety of unique properties, i.e. enhanced thermal stability of the polymer, enhanced conductivity due to denser and more ordered structure of the composite, enhanced stability of the conducting properties, and improved corrosion protection due to reduced gas permeabilty [18–25].

This study is devoted to the investigation of the formation of nanocomposites of polypyrrole with vermiculites, i.e., the possibility of inserting polymer chains into the interlayer space of these sheet silicates by in situ chemical polymerization of monomeric pyrrole taken up from the vapour phase. Two different vermiculites from Spain were chosen as starting materials, one from Santa Olalla, Huelva, (VSO) and the other one from Ojén, Málaga, (VOj). These two vermiculites mainly differ in their layer charge, which is high for the vermiculite from Santa Olalla and low for that from Ojén.

In the past, the preparation of PPy-clay nanocomposites has been achieved mainly by incorporation of the solid during in situ chemical or electrochemical polymerization of the monomers [21–24]. Only in two papers it has been shown that the oxidizing power of Fe^{3+} in the interlayer space can be used to trigger the formation of polypyrrole [19, 25]. However, the vermiculites already contain Fe^{3+} in the octahedral layer and these Fe^{3+} ions may be sufficient to induce oxidation and subsequent in situ polymerization of pyrrole even in the absence of Fe^{3+} in the

* Author for correspondence: veronica@icmse.csic.es

1388–6150/$20.00

Akadémiai Kiadó, Budapest, Hungary
Springer, Dordrecht, The Netherlands

interlayer space. In order to elucidate the importance of both the interlayer and structural Fe^{3+}, we have investigated the behaviour of vermiculites with Na^{+}, Mg^{2+} and Fe^{3+} as interlayer cations.

This paper presents a report on the characterization of the vermiculites before and after pyrrole exposure by DTA-TG, XRD, FTIR and Mössbauer spectroscopy. The latter method gives insight how strongly iron is involved in the polymerization of the pyrrole.

Experimental

Materials

For the purpose of this study, two different vermiculites from Spain were selected: VSO and VOj, with layer charges of 0.77 and 0.53, respectively. The half unit cell composition is $Mg_{0.385}(Si_{2.69}Al_{1.31})(Mg_{2.48}Al_{0.15}Fe^{3+}_{0.33}Fe^{2+}_{0.03}Ti_{0.01})O_{10}(OH)_2$ for Santa Olalla and $Mg_{0.265}(Si_{2.83}Al_{1.17})(Mg_{2.01}Al_{0.2}Fe^{3+}_{0.40}Fe^{2+}_{0.16}Ti_{0.14})O_{10}(OH)_2$ for Ojén [26]. The vermiculites were used as powder samples with a particle size <80 μm obtained by grinding in a Knife-mill (Netzsch ZSM-1, Germany).

From the original powder samples containing Mg^{2+} as interlayer cations, specimens saturated with Na^{+} and Fe^{3+} interlayer cations were prepared. The sodium saturated samples (Na-VSO and Na-VOj) were prepared by repeated treatment of the natural Mg^{2+}-vermiculites with 1 M NaCl (Aldrich) solution under refluxing conditions until the cation exchange was complete. The saturated samples were washed with distilled water until the supernatant solution became free of Cl^{-}.

The iron saturated samples (Fe-VSO and Fe-VOj) were prepared by treatment of sodium exchanged samples, previously washed with methanol, with a 0.1 N $FeCl_3 \cdot 6H_2O$ (Riedel de-Haën) solution in methanol (Aldrich) under vigorous stirring for 48 h. The procedure was repeated six times.

The exposure of the vermiculites to pyrrole (98%, Aldrich) was carried out in darkness via the vapour phase in an evacuated desiccator at room temperature. The reaction time was between one and seven days.

Methods

X-ray diffraction measurements were carried out using a Siemens Kristalloflex D-501 diffractometer at 40 kV and 40 mA with Ni-filtered CuK_α radiation and a graphite monochromator.

FTIR spectra were recorded with a resolution of 4 cm^{-1} in transmission mode in the 4000–400 cm^{-1} range with a Nicolet 510 FTIR spectometer. The spectra were obtained from KBr pressed pellets of 2 cm diameter, prepared by mixing 5 mg of sample material with 100 mg of KBr.

The differential thermal analysis (DTA) and thermogravimetric (TG) measurements were carried out at a heating rate of 6°C min^{-1} in air under normal pressure and also under N_2 flux using a Seiko TG/DTA 6300 equipment.

Mössbauer spectra were recorded at ambient temperature with a transmission spectrometer using a sinusoidal velocity waveform and a source of ^{57}Co in Rh. Isomer shifts (IS) are given with respect to the source and can be converted to shifts relative to α-iron by adding 0.11 mm s^{-1}. In order to account for distributions of the quadrupole splittings (QS) around the mean values, the spectra were fitted with Voigt profile lineshapes grouped into quadrupole doublets. Wherever warranted by an asymmetrical broadening of the doublets, a correlation between the Gaussian distribution of the QS and the IS was allowed for. Since the left components of all Fe^{3+} and Fe^{2+} doublets coincide into an unresolved peak, the IS for the two Fe^{2+} doublets required to obtain a good fit was assumed to be the same. In some cases, texture effects had to be allowed for.

Results and discussion

Figures 1 and 2 show the XRD patterns of original Mg-forms of the vermiculites (VSO and VOj) before and after exposition to pyrrole vapour. The absence of a change in the interlayer distance shows, that no intercalation of pyrrole and/or formation of PPy in the

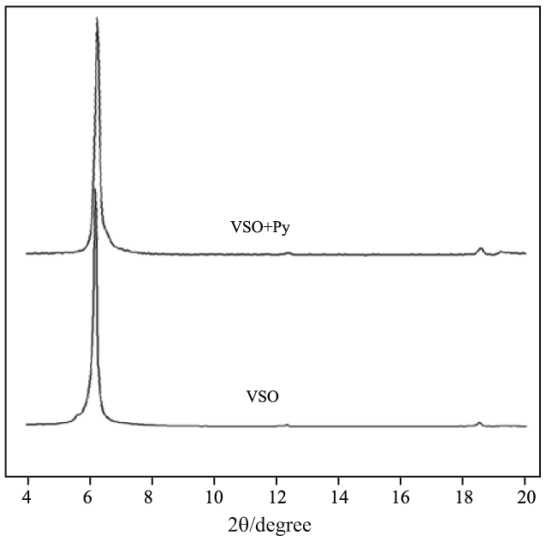

Fig. 1 X-ray diffraction patterns of the magnesium forms of the Santa Olalla vermiculite before (VSO) and after pyrrole vapour exposure (VSO+Py)

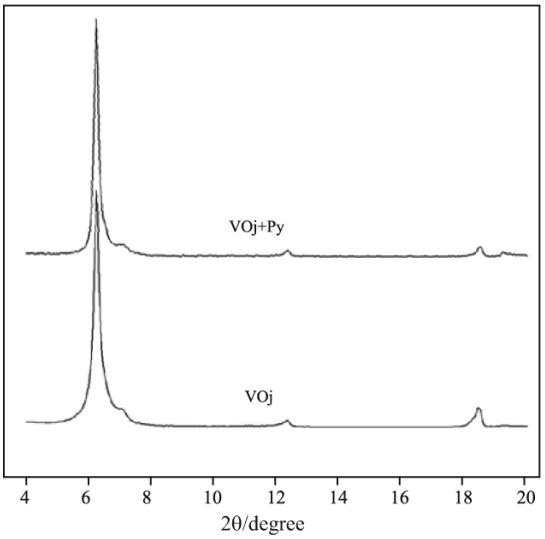

Fig. 2 X-ray diffraction patterns of the magnesium form of the Ojén vermiculite before (VOj) and after pyrrole vapour exposure (VOj+Py)

interlayer space have taken place. These results do not rule out the formation of PPy on the external surfaces of the clay particles. Indeed, after exposure to pyrrole vapour the colour of the vermiculites had changed to steel blue or even black, which is a sign of some pyrrole polymerization.

In the infrared spectral region between 1700 and 1300 cm^{-1}, characteristic of the polypyrrole formation, the band at 1630 cm^{-1} is assigned to the interlayer water molecules of vermiculite (δ_{HOH}) (Figs 3a and 4a). After the exposure to pyrrole vapour the infrared spectrum of VSO (Fig. 3b) exhibits a broad band at 1646 cm^{-1} assigned to the $\upsilon_{C=C}$ of the pyrrole monomer, which indicates that the original vermiculite adsorbs pyrrole. Probably this band overlaps with that of vermiculites at 1630 cm^{-1} (δ_{HOH}) as a

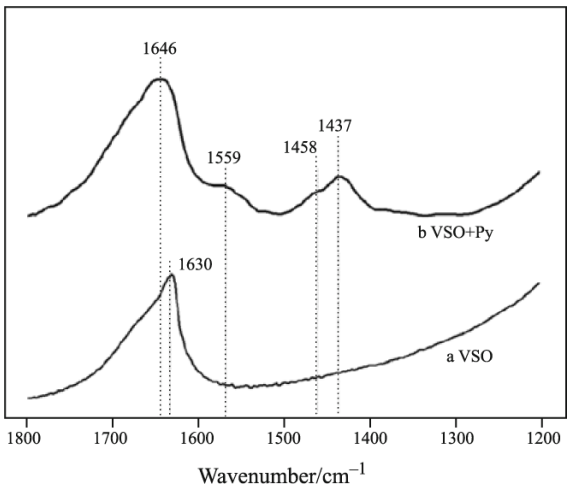

Fig. 3 IR spectra of the magnesium form of the Santa Olalla vermiculite a – before and b – after pyrrole vapour exposure

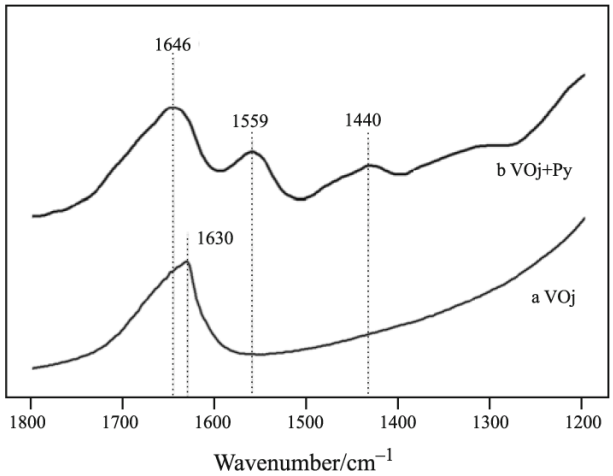

Fig. 4 IR spectra of the magnesium form of the Ojén vermiculite a – before and b – after pyrrole vapour exposure

consequence of remaining water molecules. Together with the monomer infrared band, a shoulder around 1559 cm^{-1} associated with the $\upsilon_{C=C}$ vibration modes of PPy chains is observed [19, 25, 27]. This indicates that some polymerization of pyrrole takes place. Additionally a broad band which can be resolved in two at 1458 and 1437 cm^{-1} appears in the IR spectrum. The $\upsilon_{C=N}$ symmetric and $\upsilon_{C=N}$ antisymmetric characteristic vibration modes of the pyrrole molecule appear at 1469 and 1417 cm^{-1}, respectively; a broadening and slight frequency shifts of these bands are typical for PPy formation [25]. Thus the IR bands at 1458 and 1437 cm^{-1} corroborate the polypyrrole formation in our samples. In the IR spectrum of VOj exposed to pyrrole vapour (Fig. 4b) one finds practically the same bands as in the spectrum of VSO+Py (Fig. 3b), indicating the presence of both the monomer and the polymer after pyrrole contact with the vermiculite. Considering the XRD and IR data we conclude that pyrrole is adsorbed and polymerized on the external surfaces of the particles of both vermiculites.

Figure 5 shows the TG-DTG curves taken in air for the Santa Olalla vermiculite before (a) and after pyrrole exposure (b), respectively. The parent VSO looses a total of about 16 mass% in two steps, one from 20 to 160°C (about 11%) and the other from 160 to about 300°C (about 5%). These mass losses are due to the evaporation of the interlayer water [28, 29]. The continuous mass loss between 300 and 700°C is due to the evaporation of some remaining water and to the beginning of dehydroxilation, with peaks at around 800°C [28, 29]. The DTA curve (not shown) exhibits two endothermic peaks at 144 and 240°C, also discernible in the DTG curve (Fig. 5a) and attributed to water desorption and an exothermic peak at 860°C, which indicates the formation of high temperature phases (enstatite, forsterite, spinel) depending on the interlayer cation [30].

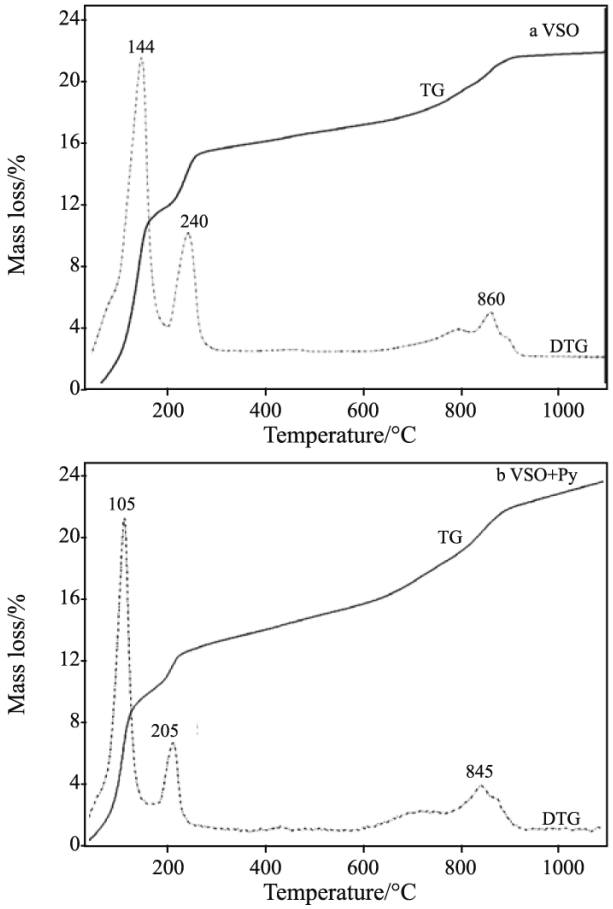

Fig. 5 TG and DTG curves of the magnesium form of the Santa Olalla vermiculite a – before and b – after pyrrole vapour exposure

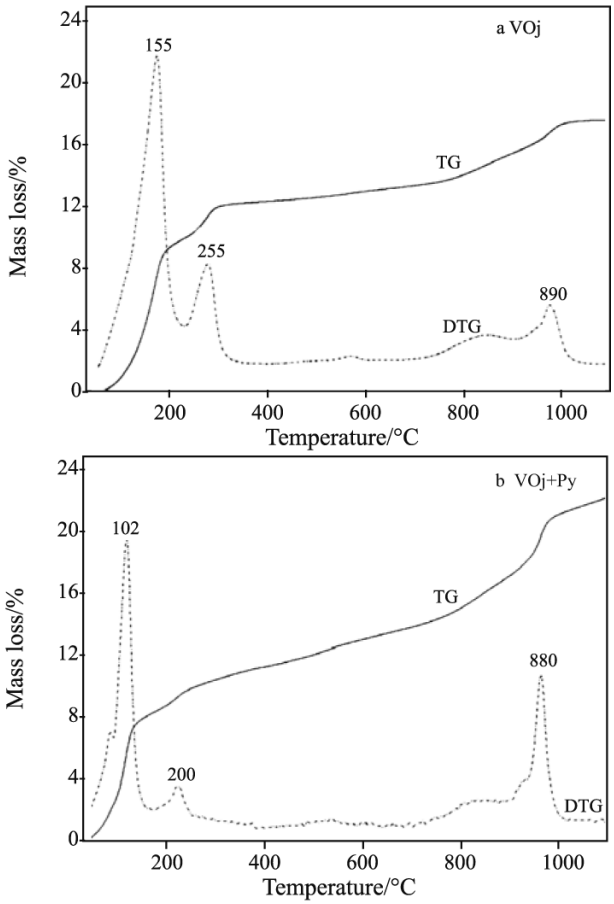

Fig. 6 TG and DTG curves of the magnesium form of the Ojén vermiculite a – before and b – after pyrrole vapour exposure

After the contact with pyrrole vapour (Fig. 5b) the TG curve exhibits practically the same mass loss steps as the parent vermiculite. The mass loss in the first and second steps is slightly lower (13%) and shifted roughly 40 °C to lower temperatures what may be due to the unusual behaviour of water–pyrrole mixtures [31]. This mass loss may be due, in addition to dehydration, to the elimination of residual pyrrole (boiling point at 130°C) [15]. Between 500 and 950°C a slightly higher mass loss (8%) takes place than in the untreated vermiculite, which can be attributed to a superposition of the dehydroxylation of vermiculite and the degradation of polypyrrole. The oxidation of PPy starts at temperatures between 200 and 300°C, depending on its resistance to oxidation [15, 24, 32]. The DTA curve (not shown) exhibits two endothermic peaks at about 105 and 205°C after pyrrole adsorption which are also seen in the DTG curve (Fig. 5b). The exothermic peak related to the formation of high temperature phases in the vermiculites around 845°C remains after the adsorption of pyrrole. The data on the thermal analysis performed under N_2 flux after pyrrole exposure did not reflect any major changes.

Figure 6a shows the TG-DTG curves obtained in air for the Ojén vermiculite before pyrrole exposure. The parent VOj loses a mass of about 9% in the first dehydration step and of about 3% in the second one, indicating a lower water content than for the Santa Olalla vermiculite. The mass loss due to dehydroxylation is about 5%. As in VSO two endothermic peaks at 155 and 255°C and an exothermic one at 890°C were observed in the DTA curve (not shown), with corresponding peaks appearing in the DTG curve (Fig. 6a). The behaviour found in the thermal analysis after pyrrole exposure is analogous for both vermiculites. Thus after pyrrole exposure the profile of the TG curve of the Ojén vermiculite also shows a three-stage weight loss with the same peaks observed in the DTG curve (Fig. 6b). In the temperature region characteristic of vermiculite dehydroxylation (450–950°C), however, the mass loss of 10% after pyrrole adsorption is almost twice as high as in the parent vermiculite. This increased mass loss can be attributed to polymer degradation. The fact that it is higher for VOj

Table 1 Mössbauer parameters for the magnesium and sodium forms of the Santa Olalla and Ojén vermiculites before and after pyrrole vapour exposure. IS (mm s^{-1}, given *vs.* the ^{57}Co: Rh source) are the isomer shifts, QS (mm s^{-1}) the electric quadrupole splittings and *A* [%] the relative areas of the different components in the spectra

Sample assignation	Fe^{3+}			Fe^{2+} site 1			Fe^{2+} site 2			ΣFe^{2+}/ %	Fe^{2+}/ Fe^{3+}
	IS	QS	A	IS	QS	A	IS	QS	A		
VSO	0.27	1.06	91.2	1.03	2.61	6.60	0.99	2.17	2.30	8.90	0.10
VSO+Py	0.28	0.97	79.0	1.02	2.60	15.3	0.90	2.38	5.70	21.00	0.27
VOj	0.27	0.99	73.7	1.03	2.58	18.0	1.00	2.13	8.30	26.30	0.36
VOj+Py	0.28	0.86	58.1	1.02	2 55	32.5	0.90	2.09	9.40	41.90	0.72
VSONa	0.27	1.06	91.2	1.03	2.61	6.60	0.99	2.17	2.30	8.90	0.10
VSONa+Py	0.28	1.06	86.2	1.00	2.57	12.3	0.90	2.06	1.60	13.90	0.16
VOjNa	0.27	0.99	73.7	1.03	2.58	18.0	1.00	2.13	8.30	26.30	0.36
VOjNa+Py	0.31	0.94	59.4	1.00	2.63	33.7	0.90	2.14	6.90	40.60	0.68

than for VSO indicates a higher amount of polymer adsorbed on VOj. The data on thermal analysis performed under N_2 flux after pyrrole exposure show a lower mass loss than in air, indicating that pyrolysis of PPy occurs instead of oxidation.

The results reported so far for the Mg form of the two vermiculites show no evidence for polypyrrole intercalation into the interlayer space, although there is evidence for the presence of polypyrrole in both vermiculites after the exposure to pyrrole vapour. The results for the Na forms are similar and will therefore not be discussed in detail.

The oxidation and subsequent polymerization of the pyrrole monomers adsorbed on the surfaces of the vermiculite particles must be caused by Fe^{3+} redox centers located in the octahedral sheet of the vermiculites. If this is the case, structural Fe^{3+} should convert to Fe^{2+} during exposure to pyrrole vapor. In order to monitor and quantify the extent of iron reduction, we have derived the Fe^{2+}/Fe^{3+} ratios for the vermiculites before and after exposure to pyrrole from room temperature ^{57}Fe Mössbauer spectra.

Table 1 contains the data resulting from the least squares fits of the Mössbauer spectra of the vermiculites before and after pyrrole exposure. The minor changes in the values for the quadrupole splittings (QS) and isomer shifts (IS) are of little importance in the present context and will not be discussed in detail. The parameters of interest are the relative areas (A) of the different iron sites and their change as a consequence of the oxidation and polymerization of pyrrole. Not unexpectedly, one observes a decrease on the area of the Fe^{3+} component on pyrrole exposure and a concomitant increase in the area of the Fe^{2+} site. The $\Sigma Fe^{2+}/Fe^{3+}$ area ratio thus increased in both vermiculites (VSO and VOj) during the pyrrole reaction, indicating the ability of the Fe^{3+} ions in the octahedral sheet to oxidize the pyrrole molecules by taking up electrons. Considering the decrease of the relative area of the Fe^{3+} component on pyrrole exposure (from 91 to 79% for VSO and from 74 to 58% for VOj), one finds that the Ojén vermiculite is more strongly reduced than the Santa Olalla vermiculite. With the total iron content of VOj being higher than that of VSO according to the half cell formulas, the total amount of iron reduced during pyrrole exposure is about twice as large for VOj than for VSO. Thus the content in polypyrrole adsorbed per formula unit on the Ojén vermiculite is expected to be higher than on the Santa Olalla vermiculite, in agreement with the thermal analysis data.

For the Na form of both vermiculites, the reduction of Fe^{3+} during exposure to pyrrole is less than for the respective Mg forms (Table 1). For the Na-Santa Olalla vermiculite, for instance, the relative area in the Mössbauer spectra decreases from 91% before exposure to only 86% after pyrrole exposure, compared to 79% for the magnesium form. Thus the extent of polymerizaton should be higher with Mg^{2+} than with Na^{+} in the interlayer space of the Santa Olalla vermiculite. The effect is not so strong for the Ojén vermiculite.

With Na^{+} or Mg^{2+} as interlayer cations, we have found no evidence for pyrrole or polypyrrole intercalation, in agreement with the absence of an increase of the interlayer spacing on pyrrole exposure, though the infrared and thermal analysis data suggest that PPy is externally adsorbed on the vermiculite particles, irrespective of the interlayer cation.

A radically different behaviour is found when Fe^{3+} ions are present in the interlayer space of the vermiculites: While the interlayer space of Fe-Santa Olalla vermiculite (Fe-VSO) is practically unchanged on pyrrole exposure (Fig. 7), the interlayer space of the Fe-Ojén vermiculite (Fe-VOj) increases by about 0.82 Å (Fig. 8), indicating the presence of polypyrrole in the interlayer space. Both vermiculites exhibit a colour change from dark grey up to black indicating

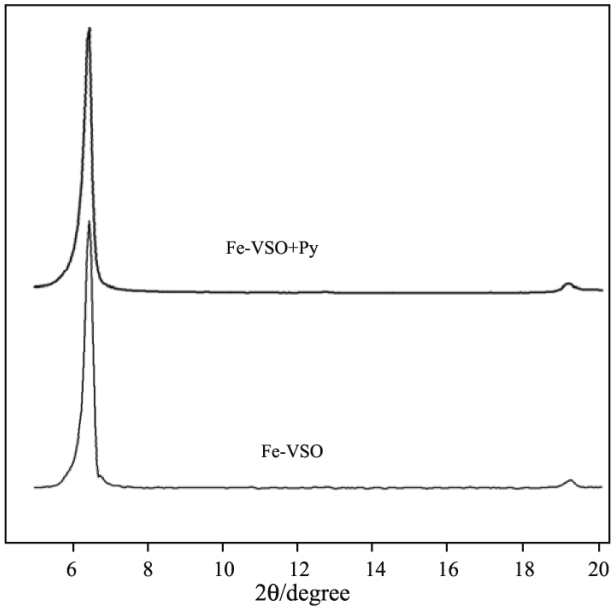

Fig. 7 X-ray diffraction pattern of Fe-Santa Olalla vermiculite before (Fe-VSO) and after pyrrole vapour exposure (Fe-VSO+Py)

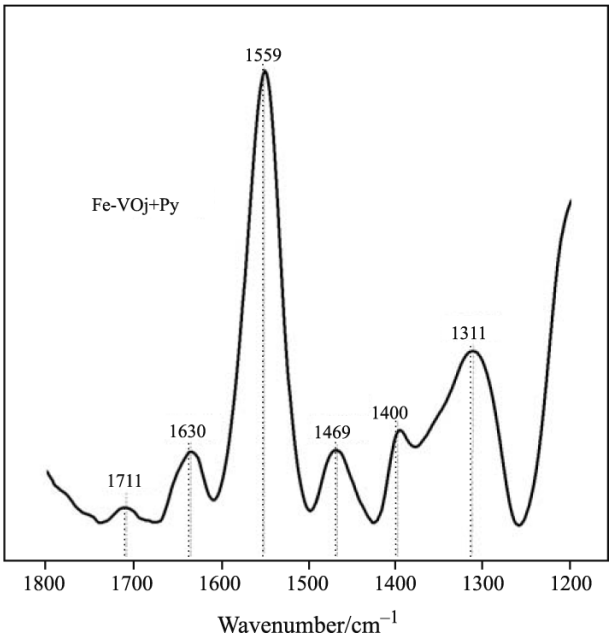

Fig. 9 IR spectrum of the Fe-Ojén vermiculite after pyrrole vapour exposure

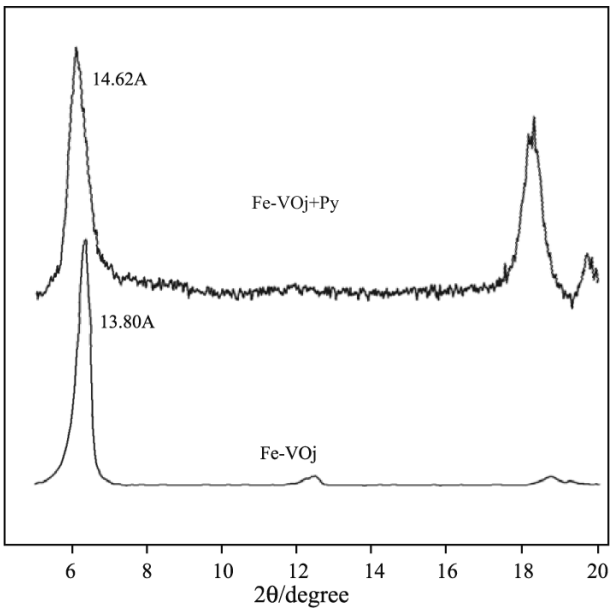

Fig. 8 X-ray diffraction pattern of Fe-Ojén vermiculite before (Fe-VOj) and after pyrrole vapour exposure (Fe-VOj+Py)

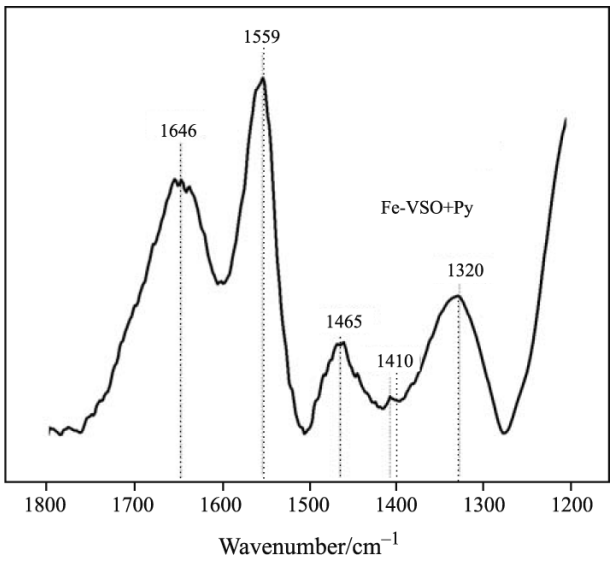

Fig. 10 IR spectrum of the Fe-Santa Olalla vermiculite after pyrrole vapour exposure

the additional presence of PPy on the external surfaces of the particles.

In the IR spectrum of Fe-VOj after pyrrole exposure (Fig. 9) the most intense band is the one corresponding to the $\upsilon_{C=C}$ vibration modes of PPy chains at 1559 cm^{-1} [19, 25, 27]. Other characteristic bands of PPy also appear, the $\upsilon_{C=N}$ symmetric and the $\upsilon_{C=N}$ antisymmetric vibration modes at 1469 and 1400 cm^{-1} confirming the polymer formation. Another band at 1311 cm^{-1} also confirms the polymerization of the monomer [18]. The weak band at around 1700 cm^{-1} is associated with the formation of products due to a partial overoxidation of PPy [19]. The IR band of pyrrole monomers at 1646 cm^{-1} is hardly discernible in the Fe-VOj infrared spectrum, indicating that monomers are virtually absent. In addition, the band at 1630 cm^{-1} associated with remaining water molecules appears in the spectrum. In the IR spectrum of Fe-VSO after pyrrole exposure (Fig. 10) one finds the characteristic PPy bands assigned to the $\upsilon_{C=C}$ and $\upsilon_{C=N}$ vibrational modes, together with the band at around 1320 cm^{-1} indicative of polymerization. Thus

the IR data confirm the notion of external surface polymerization in Fe-VSO. An intense band at 1646 cm^{-1} corresponding to the $\upsilon_{C=C}$ vibration mode of pyrrole is observed showing the presence of monomer and polymer molecules. This band probably includes the band assigned to the remaining water.

In the DTG curve of Fe-VSO heated in air after pyrrole vapour exposure a strong peak is observed at 120°C (Fig. 11a), which finds a correspondence in an endothermic peak in the DTA curve (not shown) below 200°C. This feature is attributed to the desorption of the remaining pyrrole (Boiling point 130°C) and water. In the TG curve the estimated mass loss below 200°C is about 10%. Between 200 and 900°C two strong peaks appear in the DTG curve. The first peak at around 475°C (Fig. 11a) corresponds to a weak exothermic peak in the DTA curve, which can be attributed to oxidation of PPy. The second peak at about 845°C is characteristic of the vermiculite. It corresponds to an exothermic DTA peak and is attributed to the final step of dehydroxylation followed by recrystallization into high temperature phases. Between 200 and 900°C there is a substantial mass loss of about 18%. This mass loss will be the sum of PPy oxidation and the dehydroxylation of the vermiculite, as well as the elimination of residual carbon. Under N_2 atmosphere (Fig. 11b) the TG curve of Fe-VSO exposed to pyrrole vapour shows a mass loss between 200 and 900°C that is lower by about 10% than the one observed in air. Since this mass loss is slow and rather continuous, no distinct peak is observed in either the DTG or the DTA curve, with the exception of that of vermiculite recrystallization at about 845°C. The continuous mass loss must be due to PPy pyrolysis and to vermiculite dehydroxylation.

Figure 12a shows the TG and DTG curves of Fe-VOj heated in air after pyrrole vapour exposure. This curve is different from all the curves shown previously, where the polymer was only adsorbed externally. At low temperature a peak is observed around 70°C in the DTG curve, and the DTA curve (not shown) shows a corresponding endothermic peak. The corresponding mass loss is about 2% and attributed to desorption of methanol (boiling point 65°C). A mass loss of about 7%, takes place between 200 and about 600°C. In this region two peaks near 430 and

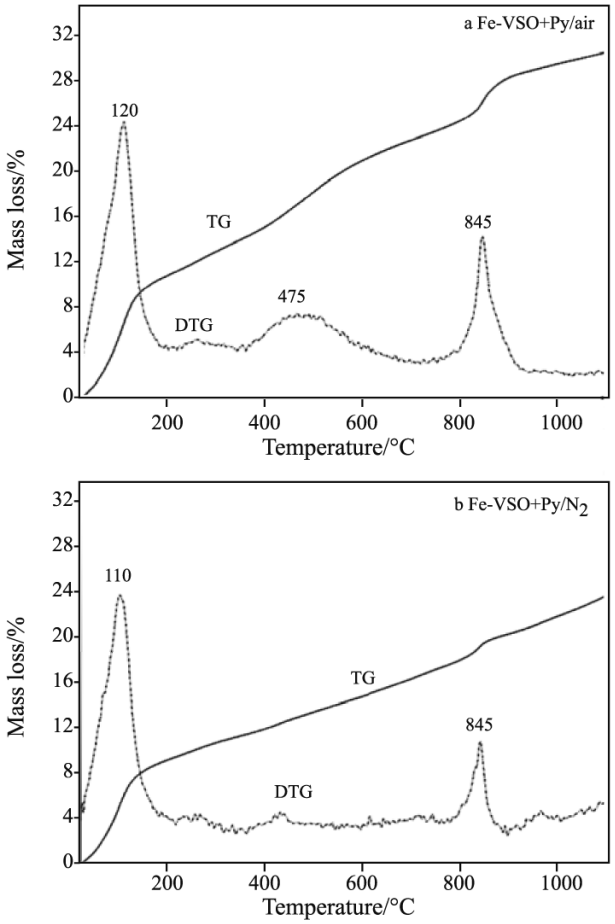

Fig. 11 TG and DTG curves of the Fe-Santa Olalla vermiculite after pyrrole vapour exposure taken in a – air and b – under N_2 atmosphere

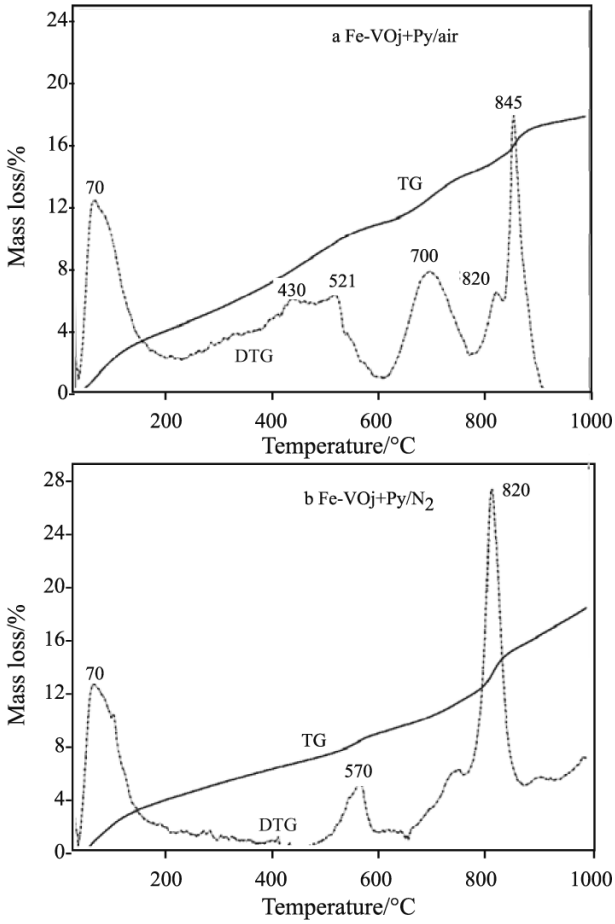

Fig. 12 TG and DTG curves of the Fe-Ojén vermiculite after pyrrole vapour exposure taken in a – air and b – under N_2 atmosphere

Table 2 Mössbauer parameters for the Fe-Santa Olalla and Fe-Ojén vermiculites before and after pyrrole vapour exposure. IS (mm s^{-1}, given *vs.* the ^{57}Co: Rh source) are the isomer shifts, QS (mm s^{-1}) the electric quadrupole splittings and *A* [%] the relative areas of the different components in the spectra

Sample assignation	Fe^{3+}			Fe^{2+} site 1			Fe^{2+} site 2			ΣFe^{2+}/ %	Fe^{2+}/Fe^{3+}
	IS	QS	A	IS	QS	A	IS	QS	A		
VSO	0.27	1.06	91.2	1.03	2.61	6.60	0.99	2.17	2.30	8.90	0.10
Fe-VSO	0.26 0.27	1.17 0.68	46.9 46.3	1.02	2.44	5.80	0.83	2.13	1.00	6.80	0.07
Fe-VSO+Py	0.26	0.84	74.2	1.01	2.56	21.5	0.90	1.99	4.30	25.80	0.35
VOj	0.27	0.99	73.7	1.03	2.58	18.0	1.00	2.13	8.30	26.30	0.36
Fe-VOj	0.29 0.26	1.02 0.61	54.9 25.3	1.03	2.59	10.3	0.90	2.55	9.50	19.80	0.25
Fe-VOj+Py	0.31 0.25	1.09 0.70	31.6 36.7	1.00	2.62	20.1	1.00	2.20	12.1	32.20	0.47

520°C can be identified in the DTG curve. These peaks can be attributed to the oxidation of the intercalated PPy [33]. The intense peak at around 700°C in the DTG may be assigned to the final stage of polymer decomposition or the elimination of the residual carbon [24]. In the range 775–900°C the DTG curve exhibits two peaks with very little mass loss that can be associated to the crystallization of new phases. The temperatures at which the PPy decomposes are higher for Fe-VOj than for the other cases. This can be explained by the difficulty for oxygen to penetrate into the interlayer space and for the volatile decomposition products to get out [4].

When the pyrrole treated Fe-VOj is heated in an N_2 atmosphere, the mass loss below 200°C (Fig. 12b) is the same as during heating in air, as would be expected for the evaporation of the residual methanol. Between 200 and 600°C the mass loss of about 4.5% is lower than during heating in air and corresponds to pyrolysis of the polymer. Between 600 and 800°C there is a mass loss of around 6% which can be due to remaining polymer molecules decomposition. At around 820°C the characteristic DTG peak attributed to vermiculite recrystallization is found as expected.

To study the influence of Fe^{3+} occupying interlayer as well as structural sites on the pyrrole adsorption and subsequent polymerization Mössbauer spectra were taken at room temperature for the Fe-VSO and Fe-VOj samples before and after exposure to pyrrole vapour. The corresponding data are given in Table 2. The discussion of these data will again be restricted to the relative areas obtained for the different iron components; a more detailed discussion can be found in [34]. After pyrrole vapour exposure, the Fe^{2+}/Fe^{3+} ratio shows an increase from 0.07 to 0.35 for Fe-VSO and from 0.25 to 0.47 for Fe-VOj. This indicates a strong reduction of the Fe^{3+} going along with the oxidation and polymerization of pyrrole. The Fe^{2+}/Fe^{3+} ratios (Tables 1 and 2) for VSO increase with the interlayer cation in the sequence Na<Mg<Fe. In the case of VOj the Fe^{2+}/Fe^{3+} ratio increases by a factor of about two independently of the interlayer cation. This seems to be in conflict with the observation of a higher degree of polymerization in case of the Ojén samples as observed in the IR spectra and the TG/DTG data. To resolve this puzzle we suggest that in the Ojén samples with the lower layer charge more pyrrole is intercalated and the oxidation/polymerization occurs mainly in the interlayer space due to catalytic effects in the constrained space.

Conclusions

Oxidative chemical polymerization of pyrrole takes place in both studied vermiculites (VSO and VOj) independently of the layer charge and structural composition of the clay and of the interlayer cation. When sodium or magnesium are the interlayer cations, pyrrole is adsorbed on the external surface. Its polymerization is incomplete, and monomeric and polymeric pyrrole coexist. One therefore cannot consider the products as proper PPy-vermiculite nanocomposites. For the formation of real PPy-vermiculite nanocomposites, i.e. of polymer chains inserted into the interlayer space, the presence of an interlayer cation with redox properties (Fe^{3+}) is required. However, the Fe-Santa Olalla and Fe-Ojén vermiculites show a different behaviour on pyrrole adsorption, with the intercalation taking place preferentially for Fe-VOj. This may be due to the different layer charge of the two vermiculites. The lower charge of the Ojén vermiculite may favour the uptake of monomeric pyrrole into the interlayer space and its subsequent polymerization.

One property of polymer-clay nanocomposites is the increase in the onset of the degradation temperature observed in TG experiments [35]. In the vermicu-

lites the onset temperature of polypyrrole degradation is at around 275°C according to the TG curves of the pyrrole treated Fe-Ojén vermiculite (Figs 12a and b), whereas thermal decomposition of pristine polypyrrole starts at 180–237°C [11]. This is only a moderate increase in the degradation temperature, perhaps because a considerable amount of the PPy is deposited on the external surface of the vermiculite.

References

1 A. Blumstein, Bull. Soc. Chim., 5 (1961) 899.
2 T. J. Pinnavaia and G. W. Beall, Eds, Polymer-clay Nanocomposites, John Wiley and Sons, 2000.
3 E. Ruiz-Hitzky and P. Aranda, Polymer-clay Nanocomposites. T. J. Pinnavaia and G. W. Beall, Eds, John Wiley and Sons, 2000, pp. 19–46.
4 E. Ruiz-Hitzky and A. V. Meerbeek, Handbook of Clay Science. F. Bergaya, G. Lagaly and B. G. K. Theng, Eds, Elsevier, 2006, pp. 583–623.
5 G. G. Wallace, G. M. Spinks and P. R. Teasdale, Intelligent Materials Systems, Technomic. Lancaster 1997.
6 P. Pfluger, M. Krounbi, G. B. Street and G. J. Weiser, Chem. Phys., 78 (1983) 3212.
7 A. Deronzier and J. C. Moutet, Acc. Chem. Res., 22 (1989) 249.
8 C. Ehrenbeck and K. Jüttner, Electrochim. Acta, 41 (1996) 511.
9 J. Duchet, R. Legras and S. Demoustier-Champagne, Synth. Met., 98 (1998) 113.
10 E. Smela, J. Micromech. Microeng., 9 (1999) 1.
11 L.-X. Wang, X.-G. Li and Y-L. Yang,, React. Funct. Polym., 47 (2001) 125.
12 S. Hara, T. Zama, W. Takashima and K. Kaneto, Synth. Met., 146 (2004) 47.
13 M. Bazzaoui, J. L. Martins, T. C. Reis, E. A. Bazzaoui, M. C. Nunes and L. Martins, Thin Solid Films, 485 (2005) 155.
14 S. Roux, P. Audebert, J. Pagetti and M. Roche, J. Mater. Chem., 11 (2001) 3360.
15 K. Sunderland, P. Brunetti, L. Spinu, J. Fang, Z. Wang and W. Lu, Mater. Lett., 58 (2004) 3136.
16 T. Wang, W. Liu, J. Tian, X. Shao and D. Sun, Polym. Compos., 25 (2004) 111.
17 D.-V. Brezoi and R.-M. Ion, Sens. Actuators B, 109 (2005) 171.
18 G. J. F. Demets, F. J. Anaissi, H. E. Toma and M. B. A. Fontes, Mater. Res. Bull., 37 (2002) 683.
19 P. W. Faguy, R. A. Lucas and W. Ma, Colloids Surf. A: Physicochem. Eng. Aspects, 105 (1995) 105.
20 J. F. Feller, S. Bruzaud and Y. Grohens, Mater. Lett., 58 (2004) 739.
21 B. H. Kim, S. H. Hong, J. W. Kim, H. J. Choi and J. Joo, Synth. Met., 135–136 (2003) 771.
22 Y. C. Liu and M.-D. Ger, Chem. Phys. Lett., 362 (2002) 491.
23 D. P. Park, J. H. Sung, S. T. Lim, H. J. Choi and M. S. Jhon, J. Mater. Sci. Lett., 22 (2003) 1299.
24 J.-M. Yeh, C. P. Chin and S. J. Chang, J. Appl. Polym. Sci., 88 (2003) 3264.
25 S. Letaíef, P. Aranda and E. Ruiz-Hitzky, Appl. Clay Sci., 28 (2005) 183.
26 J. L. Pérez-Rodríguez, F. Carrera, J. Poyato and L. A. Pérez-Maqueda, Nanotechnology, 13 (2002) 382.
27 Y. Furakawa, S. Tazawa, Y. Fuji and I. Harada, Synth. Met., 24 (1988) 329.
28 R. C. Mackenzie, Differential Thermal Analysis, Vol. 1., R. C. Mackenzie, Ed., 1970, pp. 498–534.
29 M. C. Jiménez de Haro, L. A. Pérez-Maqueda, E. T. Stepkowska, J. M. Martinez and J. L. Pérez-Rodríguez, J. Therm. Anal. Cal., 71 (2003) 761.
30 V. Ramírez-Valle, M. C. Jiménez de Haro, M. A. Avilés, L. A. Pérez-Maqueda, A. Durán, J. Pascual and J. L. Pérez-Rodríguez, J. Therm. Anal. Cal., 84 (2006) 147.
31 W. V. Wilding, K. L. Adams, A. E. Carmichael, J. B. Hull, T. C. Jarman, K. P. Jenkins, T. L. Marshall and H. L. Wilson, J. Chem. Eng. Data, 47 (2002) 748.
32 J. C. Thiéblemont, A. Brun, J. Marty and M. F. Planche, Polym., 36 (1995) 1605.
33 A. J. Ramírez del Valle, Formación de nanocomposites de intercalación sobre Caolín de Poveda utilizando acetato amónico como intermedio de reacción, PhD Thesis, 2006, Universidad de Málaga.
34 V. Ramírez-Valle, A. Lerf, F. E. Wagner, J. Poyato and J. L. Pérez-Rodríguez, Clay Miner., (2007), in revision.
35 P. Kodgire, R. Kalgaonkar, R. Hambir, N. Bulakh and J. P. Jog, J. Appl. Polym. Sci., 81 (2000) 1786.

DOI: 10.1007/s10973-007-8734-z